Identifying Approximate Linear Models for Simple Nonlinear Systems

Lucas G. Horta* and Jer-Nan Juang†
NASA Langley Research Center, Hampton, Virginia

This paper addresses the identification (realization) of approximate linear models from response data for certain nonlinear dynamic systems. Response characteristics for several typical nonlinear joints are analyzed mathematically and represented by series expansions. The parameters of the series expansion are then compared with the modal parameters of a linear model identified by the eigensystem realization algorithm. The agreement of the identified model and the analytically derived representation is excellent for the cases studied. Also, laboratory data from a model exhibiting stiffening behavior was analyzed using the eigensystem realization algorithm and fast Fourier transform. The laboratory experiment demonstrated the ability of the technique to recover the model characteristics using real data.

Introduction

An accurate analytical model that relates a system input vector to a system output vector is required for many dynamic systems, including structures. Such models are used for dynamic loads analyses, control design, and stability assessment. The modeling techniques are frequently based on rigid-body kinematics combined with linear stress-strain relationships for flexible bodies. However, many structural systems are either too complex or too poorly understood to be modeled accurately by this approach. All structural systems encountered in practice are nonlinear to some extent. The inherent complexity of nonlinear vibrational systems makes the purely theoretical approach difficult when deriving analytic models. Therefore, models based on, or improved using, measured quantities (for example, the inputs and outputs of the process) are needed. The current study considers the process of constructing a state-space model from experimental data, a procedure known as system realization.

Considerable progress has been made in the realization of nonlinear systems over the past two decades.[1] Identification of specific nonlinear structures and parameter estimation methods have all been studied. The choice among these various approaches for nonlinear system realization is dictated by the process and purpose of the realization. Unfortunately, most of these algorithms are, in general, difficult to implement or apply only to a narrow class of systems. Since identification methods for linear systems are well established and have been widely applied, the question arises as to whether a nonlinear system can be represented by a linear model that approximates the dynamic behavior of the system.

The objective of this paper is to demonstrate that an approximate linear state-space model can be constructed for nonlinear systems directly from response data. Note that this approximate linear model is input dependent. This extends the work of Ref. 2. For moderate system nonlinearities, a single model for a specific input may be adequate for acceptable response prediction. To achieve this objective, the following steps are taken. First, analytical solutions in terms of a series expansion of sine and cosine functions are derived for the system response of different kinds of simple nonlinear structures. Note that a system response representation in terms of a sine and cosine series is equivalent to a linear model in modal space characterized by the frequencies and coefficients of the series. Second, the simulated free responses of simple generic nonlinear structures are used by the eigensystem realization algorithm (ERA)[3] to construct an approximate linear model. The realized linear model has the same input/output dynamic characteristics of the original system at the measurement points. The successful application of a similar realization procedure to a nonlinear system was reported in the area of chemical processes.[4] Third, the parameters of the analytical series representation are compared with the ERA realized modal parameters. Finally, an application of this process to laboratory data for a nonlinear torsion model is included. The synthesized response data using the ERA-identified parameters are compared with the actual data in terms of Fourier transforms in amplitude and phase.

Nonlinear proportionality of restoring forces in response to certain input forces is a very common phenomenon observed in structures. To simulate, to a limited extent, the responses of simple structural systems containing nonlinearities, several single degree-of-freedom (SDOF) analytical models of hypothetical generic structural joints are formulated. Cases with multilinear, dead-band, plastic, and cubic characteristics are considered. For each hypothetical model, a series representation of the system response is obtained and compared with the ERA realized model.

Analytical Solutions for Generic Models

Consider a joint-dominated truss structure. Because of the possibly nonlinear behavior of joints, distorted response signals will occur. These data can be used in the reconstruction of an approximate linear system such that the input/output response is matched. Certain vibrational systems such as joints can be approximated by piecewise linear characteristics. Among the most common ones are systems exhibiting stiffness behavior, as shown in Fig. 1.

SDOF Piecewise Linear Systems

For piecewise linear systems (cases 1-3, Fig. 1), the solution in each linear segment can be coupled through the terminal conditions of the previous segment, thus "bootstrapping" the solution in time until the time for a half-cycle is reached. In cases with no damping, the coupled solutions can be represented by a Fourier series expansion using the period for one cycle as the generating period. The choice of one cycle

Presented as Paper 85-0686 at the AIAA/ASME/ASCE/AHS 26th Structures, Structural Dynamics, and Materials Conference, Orlando, FL, April 15-17, 1985; received Aug. 5, 1985; revision received Jan. 2, 1986.

*Research Engineer, Structural Dynamics Branch. Member AIAA.
†Senior Research Scientist, Structural Dynamics Branch. Member AIAA.

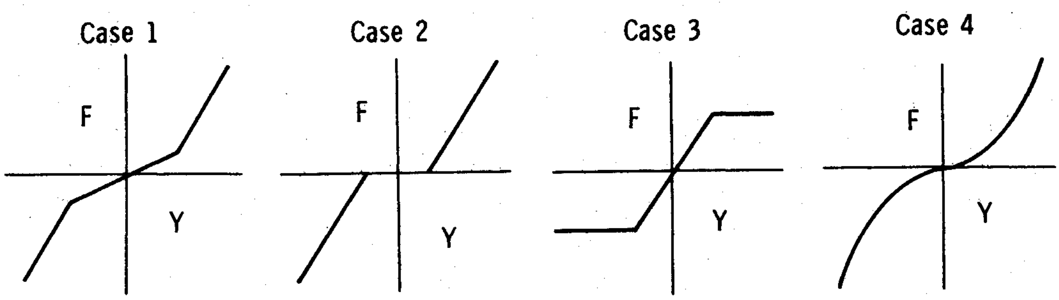

Fig. 1 Generic nonlinear structural joints.

eliminates orthogonal components and yields a representation with the simplest coordinate bases.

For example, consider the system shown in Fig. 2, which is composed of a mass M located between two linearly elastic springs $(k_1/2)$ and two noncontacting/contacting "bumper" springs[5] (k_2-k_1). The load displacement curve takes on the form shown in the upper right of Fig. 2. The governing nonlinear differential equation is

$$M\ddot{Y}+F(Y)=0 \tag{1}$$

where $F(Y)$ is a piecewise linear function of the deflection $Y(t)$. This nonlinear differential equation can be written as three linear nondimensional differential equations,

$$\begin{aligned} &\ddot{\bar{Y}}+\bar{Y}-\bar{Y}_2=0, && \bar{Y}\geq \bar{Y}_1 \\ &\ddot{\bar{Y}}+\bar{K}\bar{Y}=0, && -\bar{Y}_1\leq \bar{Y}\leq \bar{Y}_1 \\ &\ddot{\bar{Y}}+\bar{Y}+\bar{Y}_2=0, && \bar{Y}\leq -\bar{Y}_1 \end{aligned} \tag{2}$$

where $\bar{K}=k_1/k_2$. Y_2 is defined in Fig. 2 as the intersection of the upper section of the load displacement curve and the time axis. $\bar{Y}_2$ is defined as Y_2/Y_0. The initial conditions for the first equation are assumed $\bar{Y}(0)=\bar{Y}_0=1$ and $\dot{\bar{Y}}(0)=0$. The bar indicates normalization about the initial condition and the time scale $T=(M/k_2)^{1/2}$. The solution for each of these equations can be written as

$$\begin{aligned} &\bar{Y}(\bar{t})=a_1\cos(\bar{t})+b_1\sin(\bar{t})+\bar{Y}_2, && 0\leq \bar{t}\leq \tau_1 \\ &\bar{Y}(\bar{t})=a_2\cos(\bar{K}\bar{t})+b_2\sin(\bar{K}\bar{t}), && \tau_1\leq \bar{t}\leq \tau_2 \\ &\bar{Y}(\bar{t})=a_3\cos(\bar{t})+b_3\sin(\bar{t})-\bar{Y}_2, && \tau_2\leq \bar{t}\leq \tau_3 \end{aligned} \tag{3}$$

The equation constants are easily evaluated from the terminal conditions at previous times. Note that each solution holds for a certain time period. The next step is to evaluate, from the dynamics of the system, the appropriate time range for each equation. Based on Eq. (3), the time to translate the system from $\bar{Y}_0$ to $\bar{Y}_1$ assuming $\bar{Y}_0\geq \bar{Y}_1$ is

$$\tau_1=\cos^{-1}\left(\frac{\bar{Y}_1-\bar{Y}_2}{1-\bar{Y}_2}\right) \tag{4}$$

Utilizing the conditions at τ_1, the initial conditions for the second equation are $\bar{Y}(\tau_1)$ and $\dot{\bar{Y}}(\tau_1)$. Similarly, the time for the system to reach $-\bar{Y}_1$ is calculated as

$$\tau_2=-\left[\sin^{-1}\left(\frac{\bar{Y}_1}{(a_2^2+b_2^2)^{1/2}}\right)+\tan^{-1}\left(\frac{a_2}{b_2}\right)\right]\Big/\bar{K} \tag{5}$$

The third equation is initialized by the preceding terminal conditions—$\bar{Y}(\tau_2)$ and $\dot{\bar{Y}}(\tau_2)$—and the time to reach the maximum opposite displacement is

$$\tau_3=\sin^{-1}\left(\frac{\bar{Y}_2-1}{(a_3^2+b_3^2)^{1/2}}\right)-\tan^{-1}\left(\frac{a_3}{b_3}\right) \tag{6}$$

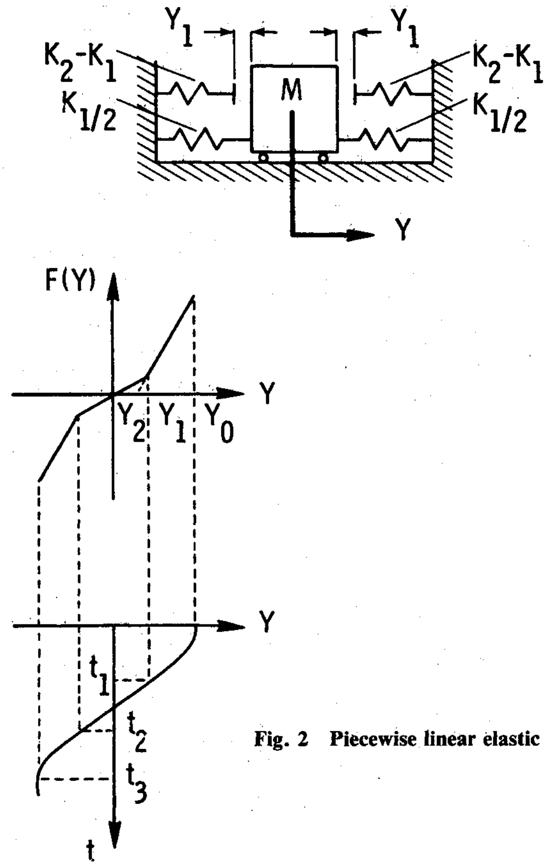

Fig. 2 Piecewise linear elastic system.

Equation (6) is used to determine the shortest possible time τ_3 for the half-period of the periodic response.

A Fourier series expansion[6] of the system response can be generated using the calculated period $2\tau_3$ and the linear solution in each time segment,

$$\bar{Y}=\sum_{n=1}^{\infty}A_n\cos\frac{n\pi t}{2\tau_3} \tag{7}$$

The Fourier coefficients are defined by

$$A_n=\frac{1}{\tau_3}\left[\int_0^{\tau_1}\bar{Y}(t)\cos\left(\frac{n\pi t}{2\tau_3}\right)\mathrm{d}t+\int_{\tau_1}^{\tau_2}\bar{Y}(t)\cos\left(\frac{n\pi t}{2\tau_3}\right)\mathrm{d}t+\int_{\tau_2}^{\tau_3}\bar{Y}(t)\cos\left(\frac{n\pi t}{2\tau_3}\right)\mathrm{d}t\right] \tag{8}$$

The sine terms do not appear because of the choice of τ_3. Observe that all the terms have a common period $2\tau_3$. These harmonics characterize the SDOF system nonlinearities. If a valid representation exits,[6] the Fourier coefficients become the modal participation factors that have to be matched by the ERA results.

The case of multilinear elastic behavior was discussed, but several other variations can be examined. For example, by

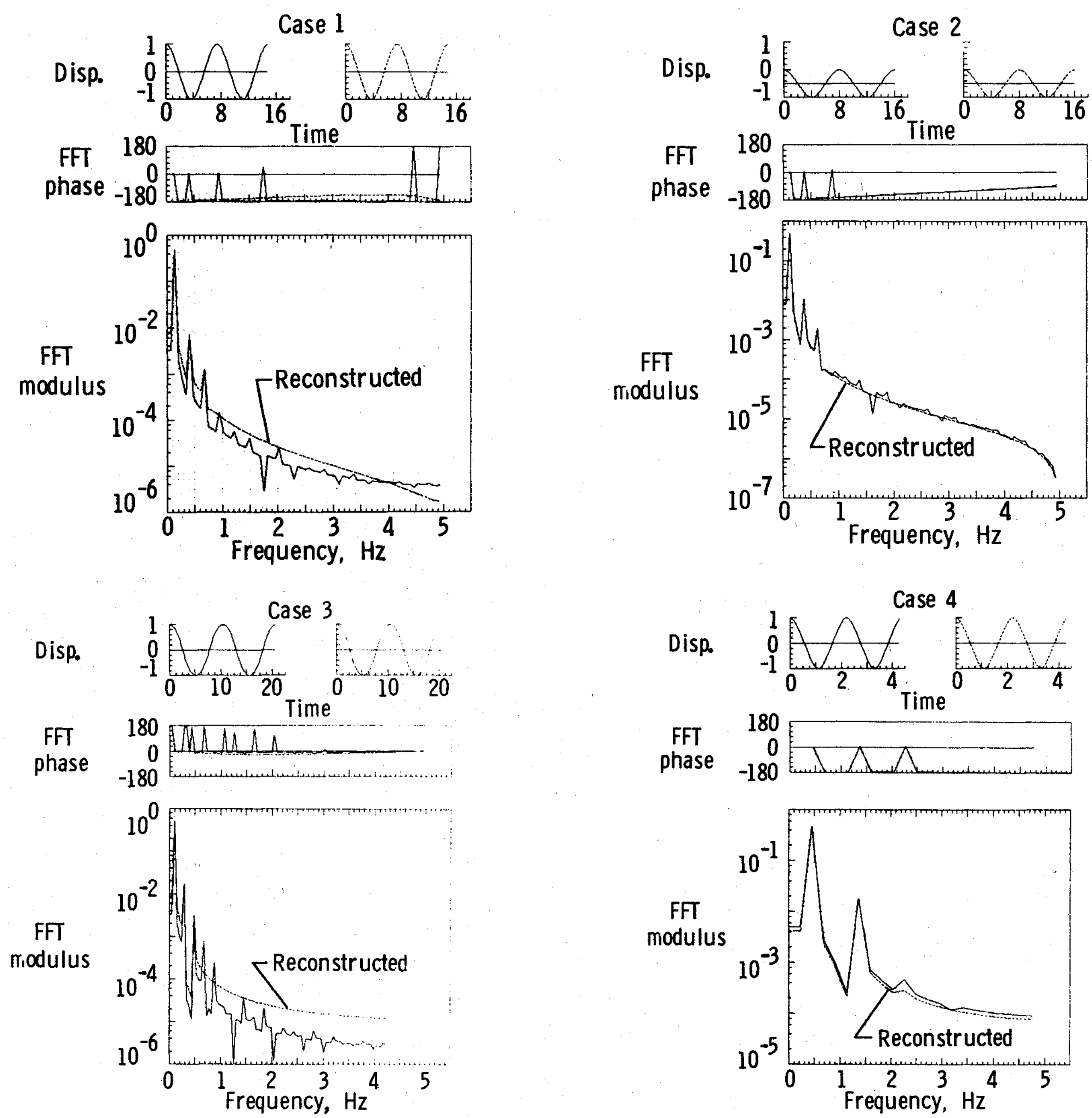

Fig 3 Comparison of ERA and FFT results for simulated data.

varying the parameters k_1 or k_2, a plastic or discontinuous linearly elastic response can be obtained; thus, the solution approach is applicable.

SDOF Cubic Case

Some structures exhibit increase in stiffness with large deformation (case 4 in Fig. 1). The strain hardening effect can be studied by assuming the reaction forces that vary as the cube of the corresponding deflection. A system with these properties is represented by the Duffing's equation as

$$\ddot{\bar{Y}}+\bar{Y}+\xi\bar{Y}^3=0 \tag{9}$$

where $\bar{Y}$ is the normalized displacement and $\xi=\bar{Y}_0^2/R$ (R is the ratio of the coefficients of the linear to cubic terms in the original equation and $\bar{Y}_0$ the initial deflection). The solution can be written in terms of elliptic functions as

$$\bar{Y}(t,\bar{Y}_0)=\frac{2\pi\bar{Y}_0}{\psi F(\pi/2,\psi)}\left[\frac{\sqrt{q}}{1+q}\cos\left(\frac{2\pi t}{P}\right)+\frac{\sqrt{q^3}}{1+q^3}\cos\left(\frac{6\pi t}{P}\right)+\ldots\right] \tag{10}$$

where

$$\psi^2=\frac{\bar{Y}_0^2}{2(\bar{Y}_0+1/\xi)}, \qquad P=\frac{4F(\pi/2,\psi)}{(\xi\bar{Y}_0+1)^{1/2}}$$

$F(\pi/2,\psi)=$ complete elliptic integral

$$q=\exp\left(\frac{-\pi[F(\pi/2,\bar{\psi})]}{F(\pi/2,\psi)}\right), \qquad \bar{\psi}=(1-\psi^2)^{1/2}$$

Again note that the harmonics with the common period P appear in Eq. (10), reflecting the nonlinear term in Eq. (9). The data supplied to the ERA method was obtained by numerical integration of the differential Eqs. (2) and (9). The ERA results are then compared with the solutions given in Eqs. (8) and (10).

SDOF Model Results

The four types of nonlinear joint stiffness variations considered in this study are shown in Fig. 1. The first case (Fig. 3, case 1) represents a structural joint with multilinear elastic response. A stiffness ratio of four (upper-to-lower amplitude

Table 1 Identified parameters for single degree-of-freedom generic structural joints

Case	Frequency, Hz		Component amplitude	
	ERA	Analysis	ERA	Analysis
1	0.135	0.134	0.986	0.987
	0.404	0.403	0.015	0.015
	0.673	0.672	−0.002	−0.002
2	0.125	0.125	0.979	0.979
	0.375	0.375	0.023	0.023
	0.625	0.625	−0.003	−0.003
3	0.096	0.096	1.030	1.030
	0.289	0.289	−0.035	−0.035
	0.482	0.482	0.006	0.006
4	0.456	0.456	0.961	0.961
	1.369	1.369	0.038	0.038
	2.281	2.281	0.001	0.001

Table 2 Laboratory experiment identified parameters

Laboratory data			Mode shape	
Freq., Hz	Damp., %	Sensor	Mag.	Phs.
1.06	0.00	1	0.0505	−48.8
		2	0.0512	−47.3
3.61	0.20	1	0.5159	−79.6
		2	0.4968	99.9
6.70	0.40	1	0.0509	89.3
		2	0.0516	89.5
10.80	0.30	1	0.0452	123.6
		2	0.0444	−60.8
12.60	0.02	1	0.0159	−36.4
		2	0.0178	147.1
15.23	0.29	1	0.0057	−67.6
		2	0.0049	115.2

region) is used and the transition region is set at 30% of the initial deflection. Using the solution procedure for piecewise linear systems, the Fourier coefficients and frequencies are compared to the eigenvalues and corresponding mode participation factors of the realized system. Note that the term "mode" is used to refer to the identified frequencies and amplitude, but is not necessarily the conventional mode definition in linear theory. Case 1 in Table 1 shows the modal amplitude, the fundamental harmonic, and the first two odd harmonics determined from Eqs. (4-8) (using a pocket calculator) and the ERA procedure (see Appendix). To compare the actual response data [numerically integrated from Eq. (2)] with the synthesized data (reconstructed using the ERA identified parameters) in terms of the frequency, amplitude, and phase, they are transformed to the frequency domain using a fast Fourier transform (FFT). The actual response data for case 1 are plotted on the upper left corner of Fig. 3 (solid line), whereas the synthesized data are plotted to the right (dashed line). The corresponding phase and modulus (half the amplitude shown in Table 1) are plotted underneath. Note that the first three peaks are matched closely by the FFT of the synthesized data. The additional peaks resulting from the FFT of the integrated data are higher harmonics that are truncated by the ERA procedure because of their small contribution. The identified parameters agree very well with the analytical solution [Eqs. (7) and (8)].

The second and third cases represent dead-band and plastic response, respectively. These two cases can be considered as variations of the previous one by changing the stiffnesses of the different sections. The transition region is again set at 30% of the initial conditions. The identified parameters for each of the two cases are shown in Table 1. The synthesized data are shown in Fig. 3. It is important to note that the initial conditions of unity are recovered by summation of the modal amplitudes.

The fourth case shown in Fig. 3 is one in which the restoring force varies with the cube of the corresponding deflection. This often occurs in strain-hardened systems or structures undergoing large deformations. For ERA analysis, the transient response of this system is generated by numerical integration of Eq. (9) with unity initial conditions and $\xi = 10$. Case 4 in Fig. 3 shows the actual synthesized response data. As in the previous cases, the first three peaks are matched closely.

All of the above cases are single degree-of-freedom analytical models describing hypothetical structural joints. Each of the series expansions [Eqs. (7) and (10)] contains harmonics with a single common period. For nonlinear stuctures with multiple degrees of freedom (MDOF), groups of harmonics with different common periods should appear in the series representation to reflect multiple nonlinearities. A MDOF nonlinear system is very difficult, if not impossible, to solve analytically. In the next section, an experiment result for a simple MDOF nonlinear system is presented using the free-decay acceleration data.

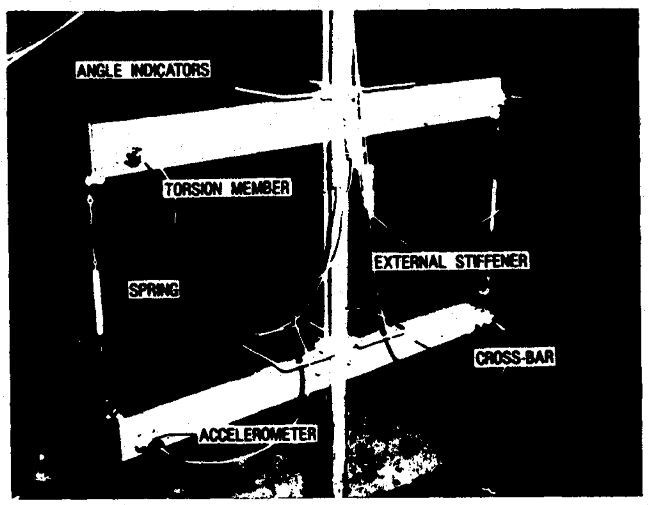

Fig. 4 Laboratory model.

Experiment Results

The laboratory experiment model shown in Fig. 4 consists of a $1 \times 1/8 \times 54$ in. aluminum torsion member, two stiff $3\frac{1}{4} \times 1 \times 36$ in. cross-bar inertia masses bolted onto the torsion member, and two springs ($K = 11.7$ lb/in.) initially loaded to 8.8 lb to restrain the out-of-phase motion of the cross bars. Since the torsion member has very small bending stiffness, an external stiffener is used to axially load the torsion member and thus reduce bending motion. The stiffener also supports two ruled angle indicators that are used to visually set the initial rotation. The system is excited by rotating one of the cross bars and then releasing it. Two servo accelerometers (Fig. 4) are used to sense the cross-bar responses. The data are digitized and then analyzed by the ERA method.

The laboratory experiment is excited by rotating the upper cross bar to 15 deg, while the lower one is held fixed. The ERA-identified parameters are shown in Table 2. Because of the complexity of the laboratory model, the identified system parameters are compared only to those obtained by the FFT. The actual responses for sensors 1 and 2 and the corresponding synthesized data are shown in Fig. 5. The six identified modes shown in Table 2 are used for reconstruction. The analyses show the first mode at 1.06 Hz corresponding to the in-phase (linear) rotational motion of the cross bars; the second mode at 3.61 Hz corresponding to the out-of-phase (nonlinear) rotational motion and the first harmonic at 10.8

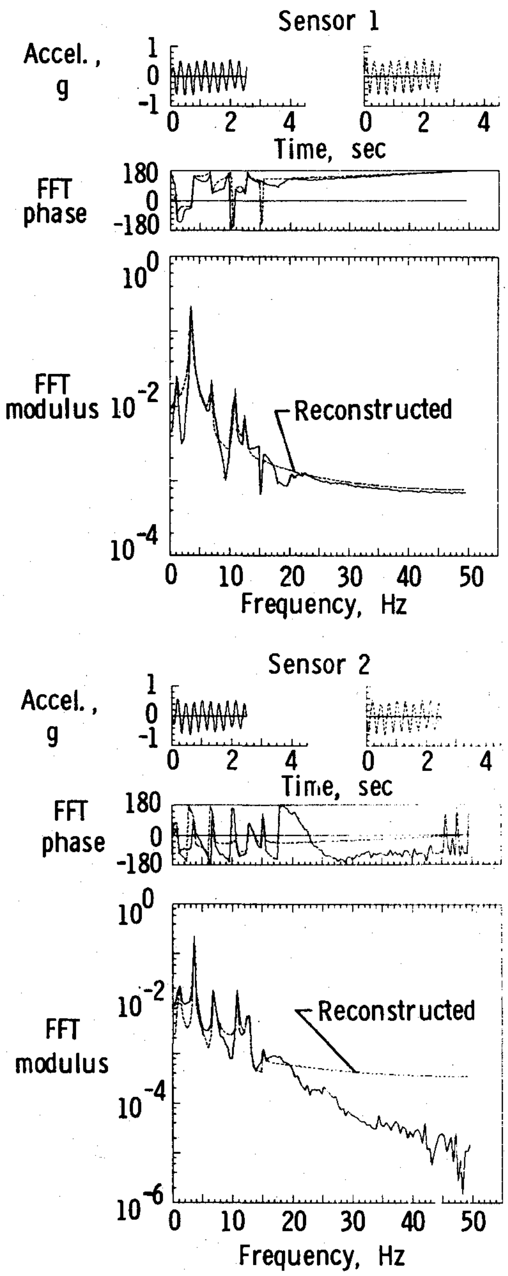

Fig. 5 Comparison of ERA and FFT results for experimental data.

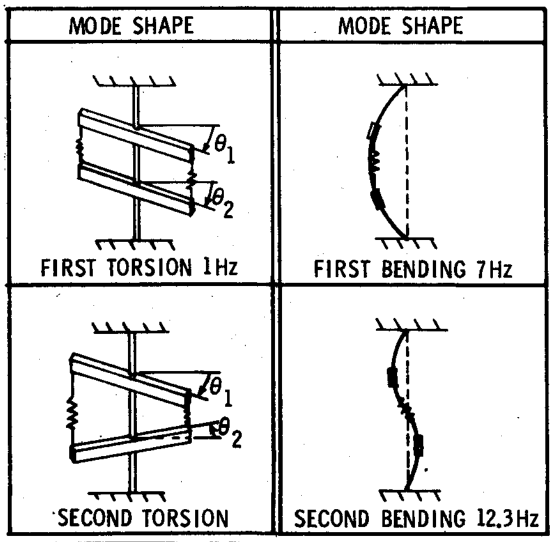

Fig. 6 Identified mode shapes for laboratory model.

Hz. Three modes due to bending of the torsion member are identified at 6.7, 12.6, and 15.23 Hz. The first six modes are matched very closely, as can be seen in Fig. 5. The first four laboratory model mode shapes are shown in Fig. 6. Observe that linear modes are identified accurately in the presence of nonlinear modes. The harmonic mode is precisely the same as the fundamental mode. This information provides a strong indication of the harmonics caused by nonlinearities. A small discrepancy in the beginning is observed, but good correlation is obtained for later times.

In general, the FFT analysis requires every component of the data to be completely periodic. Comparison in this case is good because the selection of the period for FFT analysis is obtained by observing the transient response. If the period is not properly chosen, the leakage error[7] becomes more significant, which causes the modulus to be distorted. However, the ERA analysis does not require an even period of data for accurate results.

Conclusions

Realization theory has been successfully applied to four different simulated forms of nonlinearities and a laboratory experiment. It is demonstrated that, for each of the simulated cases, the equivalent realized system possesses the same predominant characteristics as the analytically derived representation under the same initial conditions. Good correlation between the reconstructed system and laboratory data is shown. The eigensystem realization algorithm method provides a means to obtain a linear representation of a nonlinear system without a priori knowledge of the nonlinear structure of the problem.

For a linear system, distinct eigenvalues must have independent eigenvectors. If harmonically related eigenvalues have the same eigenvectors as observed in the experimental data, the system must be nonlinear. In general, both harmonics and corresponding mode shapes should be examined to assess the presence of nonlinearities. To estimate the severity, the participation factors for the harmonics should be compared to that of the fundamental mode.

Appendix: ERA Method

The following steps summarize the ERA identification procedure:

1) Construct a block Hankel matrix $H(0)$ by distributing the free decay measured data in the matrix (see Ref. 2). There are no restrictions on the number of response measurements that can be processed in a single analysis, regardless of the order of the system.

2) Decompose $H(0)$ using singular value decomposition as

$$H(0) = PDQ^T$$

where P is an orthonormal matrix of left singular vectors, Q an orthonormal matrix of right singular vectors, and D a diagonal matrix containing the singular values. No restrictions are imposed on the rank deficiency of $H(0)$.

3) Determine n, the order of the system, using the singular values greater than a prescribed error estimate.

4) Assume that there are m sensors and p inputs. Denote $E_m^T = [I_m, 0_m, 0_m \ldots]$ where I_m is an identity matrix of order m (same notation applies to E_p^T). Construct a minimum-order realization using a second block Hankel matrix $H(1)$, consisting of one data sample delay from the corresponding elements of $H(0)$, as the triple matrices

$$A = D^{-1/2} P^T H(1) Q D^{-1/2}$$

$$B = D^{1/2} Q^T E_m$$

$$C = E_p^T P D^{1/2}$$

where A is the state transition matrix, B the input matrix, and C the measurement matrix.

5) Find the eigenvalues z and the eigenvectors ψ of the realized state matrix A.

6) The modal damping rates and damped natural frequencies are simply the real and imaginary parts, respectively, of the state matrix after transformation from the z to the s plane using the relationship

$$s = \ln z / \Delta t$$

where Δt is the sampling interval.

7) The modal amplitude time histories are the rows of the matrix product

$$\psi^{-1} D^{1/2} Q^T$$

For each set of initial conditions a corresponding set of modal amplitudes is generated.

8) The desired mode shapes, or modal displacement, are the columns of the matrix product

$$E_p^T P D^{1/2} \psi$$

9) The degree to which the modes were excited by the selected initial conditions—a measure of the degree of controllability[8]—can be assessed by the purity of the modal amplitude time histories determined in step 7. One method to estimate the purity is to calculate the correlation coefficient between the identified modal amplitude history and an ideal one formed by extrapolating the initial value of the history to later points in time using the identified eigenvalue.

10) Determine the modal participation factors for each mode with respect to each sensor and each input using the entries of the input matrix B and the measurement matrix C. Let α_{ijk} be the ith sensor, jth mode, and kth input. The factor α_{ijk} can be computed by

$$\alpha_{ijk} = C_{ij} B_{jk}$$

11) The accuracy of the complete modal decomposition process can be examined by comparing the reconstructed data with the original free-response data, using various numbers of the identified modes, for example.

References

[1]Billings, S.A., "Identification of Nonlinear Systems—A Survey," *Proceedings of the Institution of Electrical Engineers,* Vol. 127, Pt. D, Nov. 1980, pp. 272-285.

[2]Horta, L.G. and Hanks, B.R. "A Study of the Effects of a Cubic Nonlinearity on a Modern Modal Identification Technique," *Proceedings of the AIAA 24th Structures, Structural Dynamics, and Materials Conference,* Pt. 2, AIAA, New York, May 1983, pp. 28-34.

[3]Juang, J.N. and Pappa, R.S., "An Eigensystem Realization Algorithm (ERA) for Modal Parameter Identification and Model Reduction," *Journal of Guidance, Control, and Dynamics,* Vol. 8, Sept.-Oct. 1985, pp. 620-627.

[4]Kallina, C., "An Approach to the Regulator Problem for Nonlinear Chemical Processes," *Proceedings of the 11th Joint Automatic and Control Conference,* Atlanta, Georgia, June 1970, pp. 329-334.

[5]Timoshenko, S., Young, D.H., and Weaver, W., *Vibration Problems in Engineering,* 4th ed., John Wiley & Sons, New York, 1974.

[6]Hildebrand, F.B., *Advanced Calculus for Applications,* Prentice-Hall, Englewood Cliffs, NJ, 1962, pp. 216-226.

[7]Richardson, M.H., "Fundamentals of the Discrete Fourier Transform," *Sound and Vibration,* March 1978, pp. 40-46.

[8]Kailath, T., *Linear Systems,* Prentice-Hall, Englewood Cliffs, NJ, 1980.